PHOTONICS Research

Robust generation of frequency combs in a microresonator with strong and narrowband loss

Jing Wang,[1,2] Zhaohong Han,[3] Yuhao Guo,[1,2] Lionel C. Kimerling,[3] Jurgen Michel,[3] Anuradha M. Agarwal,[3] Guifang Li,[1,2,4] and Lin Zhang[1,2,*]

[1]Key Laboratory of Opto-Electronic Information Technology of Ministry of Education, School of Precision Instruments and Opto-Electronics Engineering, Tianjin University, Tianjin, China
[2]Key Laboratory of Integrated Opto-Electronic Technologies and Devices in Tianjin, School of Precision Instruments and Opto-Electronics Engineering, Tianjin University, Tianjin, China
[3]Department of Materials Science and Engineering, Massachusetts Institute of Technology, Cambridge, Massachusetts 02139, USA
[4]College of Optics and Photonics, CREOL and FPCE, University of Central Florida, Orlando, Florida 32816, USA
*Corresponding author: lin_zhang@tju.edu.cn

Received 17 July 2017; revised 21 August 2017; accepted 25 August 2017; posted 30 August 2017 (Doc. ID 302256); published 11 October 2017

Octave-spanning frequency comb generation in microresonators is promising, but strong spectral losses caused by material absorption and mode coupling between two polarizations or mode families can be detrimental. We examine the impact of the spectral loss and propose robust comb generation with a loss of even 300 dB/cm. Cavity nonlinear dynamics show that a phase change associated with spectral losses can facilitate phase matching and Kerr comb generation. Given this unique capability, we propose a novel architecture of on-chip spectroscopy systems.

OCIS codes: (190.4380) Nonlinear optics, four-wave mixing; (120.4820) Optical systems; (190.3270) Kerr effect.

https://doi.org/10.1364/PRJ.5.000552

1. INTRODUCTION

Frequency comb generation in a microresonator has attracted a great deal of attention from the nonlinear optics community. It holds great potential to build compact devices for communication, frequency metrology, signal processing, and spectroscopy [1,2]. Combining highly nonlinear materials, broadband dispersion tailoring and advanced device fabrication for a high Q-factor promise octave-spanning Kerr comb generation [3–8], desirable for frequency metrology and spectroscopy. However, across such a wide band, there could often be loss mechanisms over a relatively narrow spectral region, including material absorption due to chemical bonds and impurities [9], mode coupling between polarization states [10], and mode-family crossing of the fundamental mode with a lossy higher-order mode [11,12]. The effects are deemed detrimental, causing spectrally localized Q-factor degradation, distorting mode-locked comb spectra, and limiting comb spectral broadening. However, there is little reported on how severe the problem is and how to mitigate it.

Here, we find that a strong and localized spectral loss may completely stop the generation of broadband mode-locked Kerr combs, depending on the loss bandwidth and location. We show how to eliminate the impact of strong spectral loss for stable generation of mode-locked Kerr combs with 1 THz wide spectral loss, up to 300 dB/cm, and corresponding nonlinear cavity dynamics are analyzed. With such robust comb generation, we propose a novel architecture of on-chip spectroscopy systems.

2. MODELING

We consider an Si_3N_4 microresonator as an example for Kerr comb generation. In Fig. 1, the resonator has a free spectral range (FSR) of 200 GHz, and the ring waveguide is 1680 nm × 730 nm, which is on a 3 μm SiO_2 substrate and coated by SiO_2. A bus waveguide is used to couple a pump into the cavity. Propagation loss is 0.2 dB/cm, and the coupling coefficient is 0.0037, which is in a slightly overcoupled regime, corresponding to a cavity Q-factor of 6×10^5. The dispersion property is shown in Fig. 2(a), which has two zero-dispersion wavelengths located at 1260 and 1620 nm, and we use a pump power of 700 mW at 1420 nm, which is almost the center of the anomalous dispersion region, where the dispersion is $-0.014\ \mathrm{ps}^2/\mathrm{m}$, and the nonlinear coefficient is $0.96\ \mathrm{m}^{-1}\cdot\mathrm{W}^{-1}$. The parameters used here are typical and can be easily achieved in Si_3N_4 microresonators in practice [6,13,14].

To simulate Kerr frequency comb generation, we use the Lugiato–Lefever equation as follows [7]:

$$\left[\tau_0\frac{\partial}{\partial\tau}+\frac{\alpha}{2}+\frac{\kappa}{2}-j\delta_0+jl\sum_{m=2}^{\infty}\frac{(-j)^m\beta_m}{m!}\frac{\partial^m}{\partial t^m}\right]A(\tau,t)$$
$$=\sqrt{\kappa}A_{\mathrm{in}}-j\gamma l|A(\tau,t)|^2A(\tau,t), \quad (1)$$

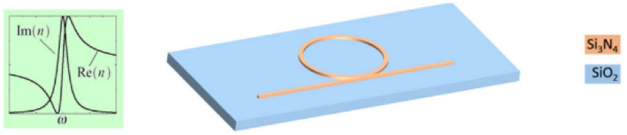

Fig. 1. Si_3N_4 cavity used for comb generation. The effective index's real and imaginary parts are governed by the Kramers–Kronig relations.

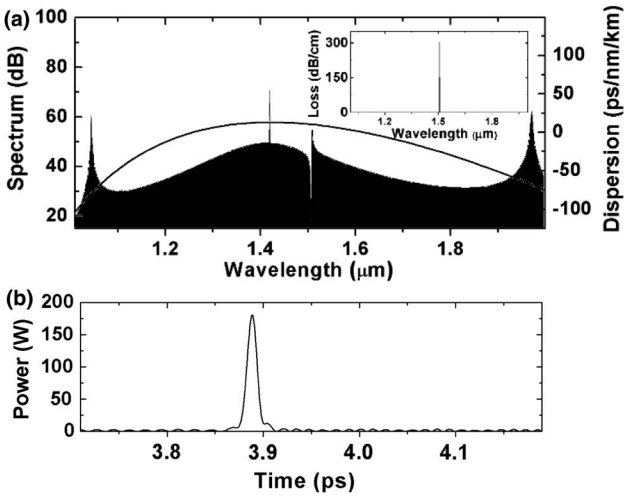

Fig. 2. Spectral loss as large as 300 dB/cm with an FWHM of 200 GHz is added to the primary comb lines closest to the pump. A mode-locked Kerr comb can be generated in (a), associated with a cavity soliton in (b). The inset in (a) shows the attenuation profile of loss peak of 300 dB/cm. The ripples on the pulse pedestal are caused by beating between dispersive waves.

where $A = A(\tau, t)$ and A_{in} are the intracavity field and the input pump field (pump power $P_{\text{in}} = |A_{\text{in}}|^2$), respectively. τ and t are the fast and slow times, respectively. τ_0 is the round-trip time, and δ_0 is the cavity phase detuning. α is the power loss per round trip, and κ is the power coupling coefficient. The all-order dispersion is used as in Ref. [15]. To add the spectrally localized loss to the device, we introduce a Lorentzian-shaped change in the imaginary part of the refractive index, determined by the specified loss value and bandwidth. According to the Kramers–Kronig relations, as shown in Fig. 1, the real part of the effective index has an additional change as well. Note that in the following sections, when we mention "loss," we actually mean the joint effects of both loss and its associated phase change.

3. RESULTS AND DISCUSSION

According to the nonlinear cavity dynamics in mode-locked Kerr comb generation, primary comb lines are first generated due to phase matching [16], which are responsible for the subsequent formation of subcombs. The suppression of the primary comb lines due to spectral loss is deemed detrimental. Thus, we first investigate the influence of the loss located at one of the nearest primary comb lines, at 1508 nm. Figure 2(a) shows the obtained comb, with a strong loss of 300 dB/cm and its full width at half

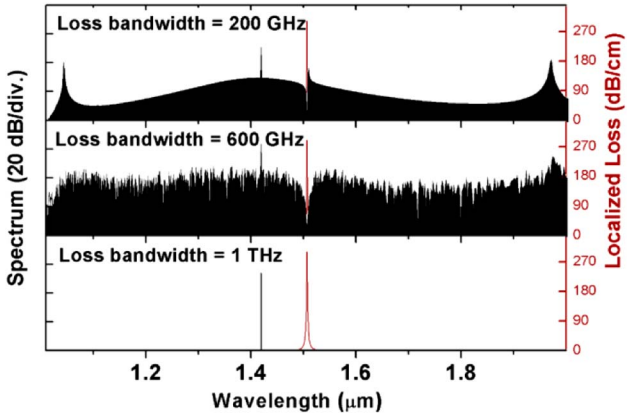

Fig. 3. Different comb generation processes are seen as the loss bandwidth increases, with the loss of 300 dB/cm at the nearest primary comb lines. The corresponding loss profiles are shown in red lines. The comb is not mode-locked anymore for a loss bandwidth of 600 GHz, while comb generation is completely stopped for a loss bandwidth of 1 THz.

maximum (FWHM) bandwidth of 200 GHz (i.e., one FSR). We can clearly see a sharp intensity dip indicating suppression of comb lines at 1508 nm in the comb spectrum, while there is a peaking effect close to the dip, as shown in previous experiments [9]. Note that the comb can still be mode-locked with such a big perturbation, showing great robustness of the comb generation. As a result, a cavity soliton can be seen in Fig. 2(b). The distortion of the soliton pulse in the time domain is believed to be caused mainly by the interference between two strong dispersive waves. We vary the loss from 3 to 30 and 300 dB/cm at 1508 nm, with the same bandwidth of 200 GHz. All the spectra can finally evolve into the mode-locked combs. The dip due to the localized loss becomes deeper with the increased loss from 0.3 to 8 and 24 dB. The comb bandwidth is not narrowed as the loss increases, showing potential for wideband comb generation under a big perturbation due to loss.

Next, we vary the bandwidth of the spectral loss with the loss peak value kept at 300 dB/cm, centered at one of the nearest primary comb lines at 1508 nm. Figure 3 shows the final spectra with the loss bandwidths of 200 GHz, 600 GHz, and 1 THz, i.e., 1, 3, and 5 FSRs, respectively. When the loss bandwidth is increased to 600 GHz, Kerr comb generation is significantly disturbed, stopped at the modulational instability stage with no mode-locked solitons formed anymore. Furthermore, when the loss bandwidth is increased to 1 THz, no comb lines can be generated on the both sides of the pump, indicating that Kerr comb generation is completely stopped, and no power is transferred from the pump to new frequencies via the primary comb lines. From above, we see that the localized loss centered at the nearest primary comb lines with a wide bandwidth can be very detrimental to Kerr comb generation. Note that here the localized loss is only added to one side of the pump, which would be the similar to the case with the loss added on the both sides, according to the symmetry of the four-wave mixing process.

In order to minimize the detrimental effect of the localized strong loss with a wide bandwidth, we examine comb generation

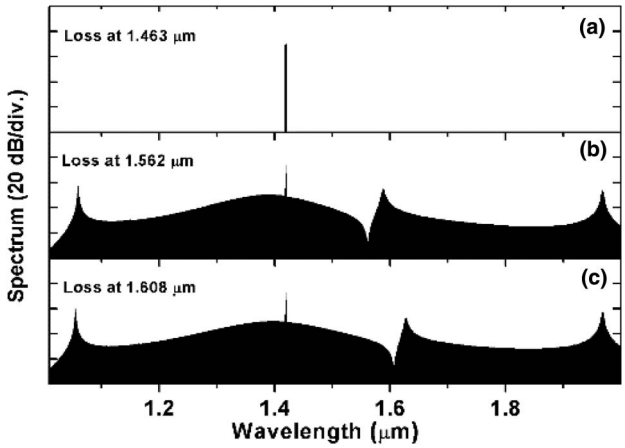

Fig. 4. Mode-locked Kerr combs are obtained as 1 THz wide loss of 300 dB/cm moves away from the pump, beyond the nearest primary comb lines. This holds even if the loss is at the second nearest primary comb line.

by shifting the loss's peak wavelength away from the nearest primary comb lines with a step of 1 THz, when the loss is 300 dB/cm and has a bandwidth of 1 THz. In Fig. 4, the disturbance induced by the strong spectral loss can completely stop the comb generation until shifting the loss peak to 1562 nm, which is about 7 THz away from the nearest primary comb lines. Despite the obvious dip caused by the localized loss, mode-locking as well as wide bandwidth can be both realized with the loss located at 1562 nm in the formed comb. We also check the influence on the comb generation, when such a loss is added on the second nearest primary comb lines at 1608 nm in Fig. 4(c). Solitons can still be formed with such a perturbation. It implies that the effective way to eliminate the detrimental effect of the spectral loss is to properly choose the pump wavelength to make sure that the nearest primary comb lines are far enough away from the loss. Once it is satisfied, the comb spectrum can extend well beyond the lossy region, still being octave-spanning.

Intriguingly, in contrast to the generated combs in Fig. 2, where the combs are mostly centered at the pump, one may note from Fig. 4 that the comb peak is shifted away from the pump. This is because the spectral loss is viewed as a perturbation to cavity soliton formation, and the soliton tends to adapt itself to survive by self-frequency-shifting away from the perturbation, similar to the mechanisms revealed in Ref. [15]. One can instead look at Fig. 4 in the following way. When the spectral loss becomes closer to the pump from Fig. 4(c) to Fig. 4(b), the soliton spectrum shifts further away. Of course, the requirement is that the nearest primary comb lines are not affected much by the loss so that a cavity soliton is successfully formed. When the loss moves closer to the pump, the primary comb lines feel strong absorption, which stops soliton formation, as in Fig. 4(a).

Examining the initial cavity dynamics reveals more details of the impact of the strong spectral loss, which in turn confirms the robustness of Kerr comb generation. Figures 5(b) and 5(c) show the initial cavity dynamics corresponding to the cases in Figs. 4(b) and 4(c), which are compared to the case without

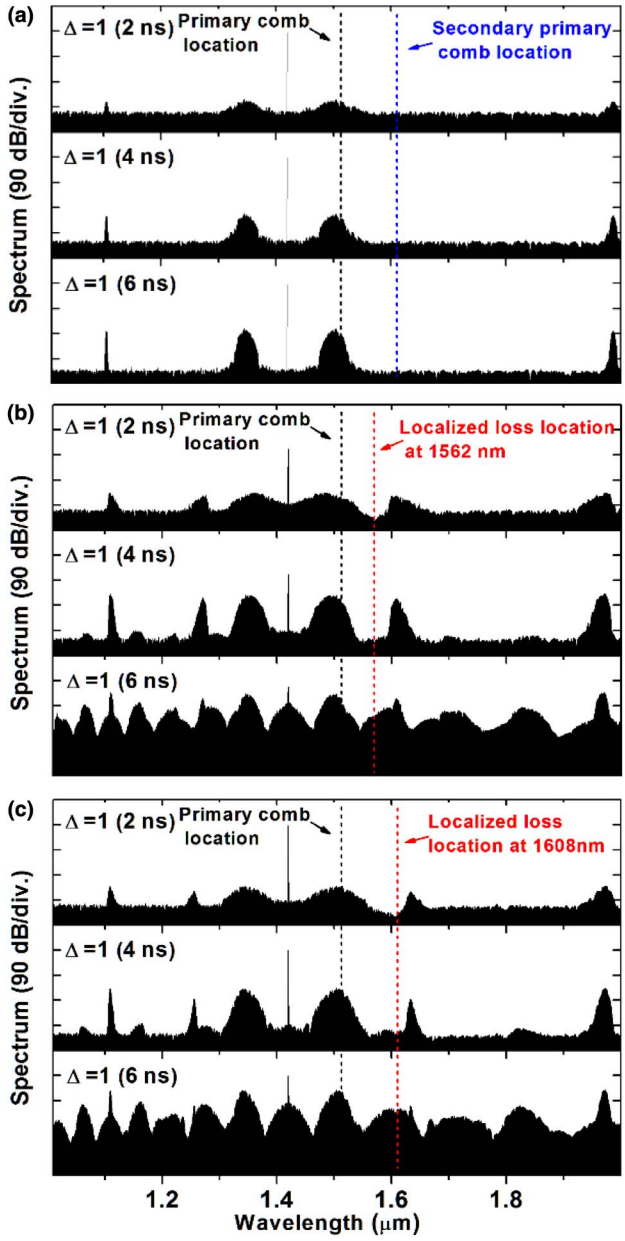

Fig. 5. Initial cavity dynamics with 300 dB/cm, 1 THz wide loss located at (b) 1562 and (c) 1608 nm. Compared to the case with no loss in (a), comb generation is enhanced in (b) and (c).

spectral loss in Fig. 5(a). The comb evolutions at 2, 4, and 6 ns are shown, as the pump laser is red-detuned away from the cold-cavity resonance by one linewidth ($\Delta = 1$). In Fig. 5(b), since the primary comb lines are affected by the loss, new frequency components grow up not exactly at the locations where the nearest primary comb lines are supposed to be. Instead, the new frequencies on both sides of the loss obtain a large gain. It is attributed to a change in the phase-matching conditions due to the modified real part of the refractive index. It confirms the robustness of Kerr comb generation. Besides, from the comparison with no loss in Fig. 5(a), sidebands grow up faster in Figs. 5(b) and 5(c), indicating the enhancement of the Kerr comb generation process.

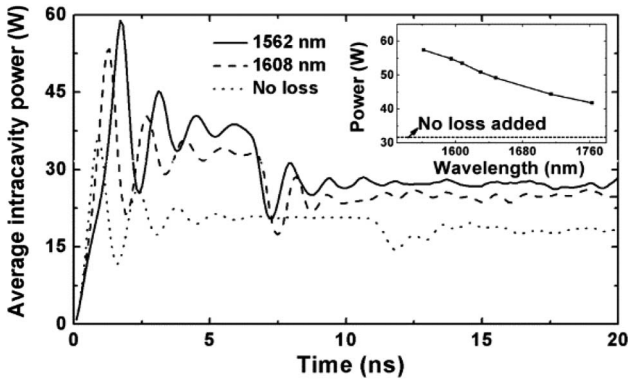

Fig. 6. Initial average intracavity power is analyzed when the loss is located at different frequencies. The peaks of the oscillating curves are extracted and plotted in the inset.

It is even more intriguing that the enhancement of initial power transfer from the pump to the primary comb lines becomes more significant as the strong spectral loss moves closer to the pump. We show the evolution of the average intracavity power in the initial 20 ns (a few times longer than the cavity photon lifetime) with the loss located at different frequencies. Note that all the loss locations are away from the primary comb lines by >7 THz, so they all finally evolve into mode-locked combs. In Fig. 6, the intracavity power experiences oscillations at the first 5 ns and becomes more stable afterwards. Compared to the case with no loss (dotted line), more power is accumulated in the cavity when the spectral loss is added. In the inset in Fig. 6, we extract the peak values of the oscillating average intracavity power in each case in the initial 20 ns. When the loss is moved from 1763 to 1562 nm, closer to the wavelength of the primary comb lines (1508 nm), the peak value of the initial average intracavity power monotonously increases from 42 to 59 W and is all above the 31.6 W in the no loss case (dashed line in the inset). This is because the additional loss is accompanied by the refractive index change in its real part, which improves the phase-matching condition. When we only modify the imaginary part of the refractive index and keep the real part unchanged, the power boost does not appear anymore.

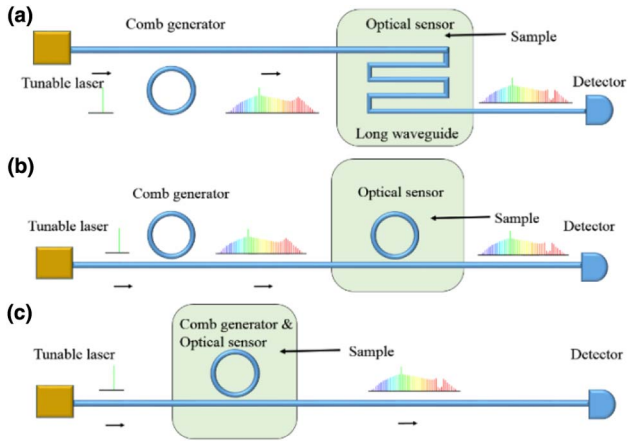

Fig. 7. Three different architectures of comb-based on-chip spectroscopy systems.

The robustness of the comb generation with a strong spectral loss could profoundly influence the architecture of an on-chip spectroscopy system. Conventionally, as shown in Fig. 7(a), a microresonator comb is transmitted through a long waveguide in a gas chamber or a microfluidic channel to increase interaction length and enhance sensing sensitivity. This requires a large chip size. Alternatively, one can fold the long waveguide into a ring cavity in Fig. 7(b) to reduce the area. However, the FSR difference of the two cavities greatly reduces the transmission of the comb. Here, the revealed robustness of mode-locked comb generation with strong localized absorption paves the way to combine the comb generator with the sensing part, in which the nonlinear cavity works as a comb generator and a sensor at the same time. As shown in Fig. 7(c), this would greatly reduce the chip size and guarantee the comb transmission as well, leading to a novel architecture of on-chip spectroscopy systems.

4. SUMMARY

We have shown the impact of the strong spectral loss on Kerr frequency combs. The comb generation can be either completely stopped or even enhanced, depending on the loss location and its bandwidth. By moving the pump to avoid the primary comb lines, it is possible to eliminate its detrimental effect. The revealed robustness of mode-locked comb generation would lead to a novel architecture of on-chip spectroscopy systems.

Funding. National Basic Research Program of China (973) (2014CB340104/3, 61775164, 61335005, 61377076, 61575142, 61431009); Advanced Integrated Optoelectronics Facility at the Tianjin University.

REFERENCES

1. J. Pfeifle, V. Brasch, M. Lauermann, Y. Yu, D. Wegner, T. Herr, K. Hartinger, P. Schindler, J. Li, D. Hillerkuss, R. Schmogrow, C. Weimann, R. Holzwarth, W. Freude, J. Leuthold, T. J. Kippenberg, and C. Koss, "Coherent terabit communications with microresonator Kerr frequency combs," Nat. Photonics **8**, 375–380 (2014).
2. T. J. Kippenberg, R. Holzwarth, and S. A. Diddams, "Microresonator-based optical frequency combs," Science **332**, 555–559 (2011).
3. Y. K. Chembo and N. Yu, "On the generation of octave-spanning optical frequency combs using monolithic whispering-gallery-mode microresonators," Opt. Lett. **35**, 2696–2698 (2010).
4. P. Del'Haye, T. Herr, E. Gavartin, M. L. Gorodetsky, R. Holzwarth, and T. J. Kippenberg, "Octave spanning tunable frequency comb from a microresonator," Phys. Rev. Lett. **107**, 063901 (2011).
5. Y. Okawachi, K. Saha, J. S. Levy, Y. H. Wen, M. Lipson, and A. L. Gaeta, "Octave-spanning frequency comb generation in a silicon nitride chip," Opt. Lett. **36**, 3398–3400 (2011).
6. S.-W. Huang, H. Zhou, J. Yang, J. F. McMillan, M. Yu, D. L. Kwong, L. Maleki, and C. W. Wong, "Mode-locked ultrashort pulse generation from on-chip normal dispersion microresonators," Phys. Rev. Lett. **114**, 053901 (2015).
7. L. Zhang, C. Bao, V. Singh, J. Mu, C. Yang, A. M. Agarwal, L. C. Kimerling, and J. Michel, "Generation of two-cycle pulses and octave-spanning frequency combs in a dispersion-flattened microresonator," Opt. Lett. **38**, 5122–5125 (2013).
8. Y. Nakagawa, Y. Mizumoto, T. Kato, T. Kobatake, H. Itobe, Y. Karinuma, and T. Tanabe, "Dispersion tailoring of a crystalline whispering gallery mode microcavity for a wide-spanning optical Kerr frequency comb," J. Opt. Soc. Am. B **33**, 1913–1920 (2016).

9. C. H. Henry, R. F. Kazarinov, H. J. Lee, K. J. Orlowsky, and L. E. Katz, "Low loss Si_3N_4–SiO_2 optical waveguides on Si," Appl. Opt. **26**, 2621–2624 (1987).
10. S. Ramelow, A. Farsi, S. Clemmen, J. S. Levy, A. R. Johnson, Y. Okawachi, M. R. E. Lamont, M. Lipson, and A. L. Gaeta, "Strong polarization mode coupling in microresonators," Opt. Lett. **39**, 5134–5137 (2014).
11. T. Herr, V. Brasch, J. D. Jost, I. Mirgorodskiy, G. Lihachev, M. L. Gorodetsky, and T. J. Kippenberg, "Mode spectrum and temporal soliton formation in optical microresonators," Phy. Rev. Lett. **113**, 123901 (2014).
12. A. A. Savchenkov, A. B. Matsko, W. Liang, V. S. Ilchenko, D. Seidel, and L. Maleki, "Kerr frequency comb generation in over-moded resonators," Opt. Lett. **20**, 27290–27298 (2012).
13. X. Xue, Y. Xuan, Y. Liu, P.-H. Wang, S. Chen, J. Wang, D. E. Leaird, M. Qi, and A. W. Weiner, "Mode-locked dark pulse Kerr combs in normal-dispersion microresonators," Nat. Photonics **9**, 594–600 (2015).
14. J. S. Levy, A. Gondarenko, M. A. Foster, A. C. Turner-Foster, A. L. Gaeta, and M. Lipson, "CMOS-compatible multiple-wavelength oscillator for on-chip optical interconnects," Nat. Photonics **4**, 37–40 (2010).
15. L. Zhang, Q. Lin, L. C. Kimerling, and J. Michel, "Self-frequency shift of cavity soliton in Kerr frequency comb," arxiv: 14014.1137 (2014).
16. T. Herr, V. Brash, J. D. Jost, C. Y. Yang, N. M. Kondratiev, M. L. Gorodetsky, and T. J. Kippenberg, "Temporal solitons in optical microresonators," Nat. Photonics **8**, 145–152 (2014).